

Effect of Ocean Iron Fertilization on the Phytoplankton Biological Carbon Pump

Adam Pan^{1,2}, Babak Pourziaei¹ and Huaxiong Huang^{1,*}

¹ Department of Mathematics and Statistics, York University, Toronto, Ontario, Canada M3J 1P3

² Program of Engineering Science, University of Toronto, Toronto, Ontario, Canada M5S 1A1

Received 11 April 2010; Accepted (in revised version) 3 September 2010

Available online 15 October 2010

Abstract. It has been proposed that photosynthetic plankton can be used as a biological carbon pump to absorb and sequester carbon dioxide in the ocean. In this paper, plankton population dynamics are simulated in a single stratified water column to predict carbon dioxide sequestering due to surface iron fertilization in deep ocean. Using a predator-prey model and realistic parameter values, iron fertilization was found to only cause temporary blooms up to 5 months in duration, and relatively small increases in adsorption of atmospheric CO₂.

PACS (2006): 87.10.Ed, 87.18.Wd, 87.23.Cc

Key words: Phytoplankton, carbon dioxide, iron fertilization, carbon pump.

1 Introduction

A recent initiative for combating climate change is using photosynthetic plankton (phytoplankton) as a biological carbon pump to absorb and sequester carbon dioxide within the ocean. Iron fertilization has the potential to dramatically increase the potency of phytoplankton blooms, leading to an increased uptake of the greenhouse gas. The use of iron fertilization in high nitrogen, low chlorophyll (HNLC) oceans has the potential to increase the carbon storage capacity of the oceans.

Plankton population dynamics have been explored quite thoroughly in the past; both in theory and practice. While experiments on small scales have proven relatively successful, increasing the carbon processing ability of phytoplankton cultures, the effect of long term iron fertilization on large oceanic blooms has remained unevaluated

*Corresponding author.

URL: <http://www.math.yorku.ca/~hhuang/>

Email: adampan@utoronto.ca (A. Pan), bobbyp@mathstat.yorku.ca (B. Pourziaei), hhuang@yorku.ca (H. X. Huang)

to date. However, several short term iron experiments have been carried out over various HNLC oceans.

More recently, the Indo-German expedition LOHAFEX [8] was carried out with the intention of testing whether iron fertilization was a feasible means of increasing phytoplankton yield of the Southern Ocean. Over 300 square kilometers of ocean was fertilized with 20 tonnes of iron sulfate. The expedition lasted 45 days. The results [10] of the expedition showed that there was little increase in overall phytoplankton population with respect to additional iron, and the researchers noted that the predator species in the system (mainly zooplankton and cephalopods) reacted to the initial spike in phytoplankton population, consuming additional phytoplankton and damping what would otherwise have been a population boom.

While iron models have already been developed [3–5], they have not been applied to the problem of evaluating iron fertilization. The existing models have only been applied to naturally occurring systems [6,7]. In addition, there is no model to describe the actual sequestering of carbon dioxide into the ocean, which currently can only be estimated from other environmental parameters. To complement the field studies currently being carried out, we use a modeling approach to further investigate the effect of iron fertilization on phytoplankton in terms of carbon sequestering.

2 Methodology

Two existing models form the basis of the mathematical model of the system. The first one, developed by Huisman et al. [3,4] gives a one dimensional stratified water column, wherein turbulent diffusion dominates above the thermocline. The Huisman model provides a good physical basis for the system, but does not take into account predator interaction. Therefore, the growth model in their model is not sufficiently realistic. The KKYS model [6], and its advancement, the KKYS-Fe model [9], on the other hand, provide the relevant biological processes including iron. As the KKYS (-Fe) models are designed to function as part of a three dimensional ecological simulation, the governing equations and thus simulation techniques used are unnecessary for the purposes of this study, and the physical model used by the KKYS-Fe model are replaced by one dimensional counterparts. Together they form the basis of the model in this paper.

2.1 Mathematical model

A single, one dimensional, stratified water column of depth z_m is assumed. Within this column, there are multiple compartments, or species, simulated. The compartments are as follows: Phytoplankton (PHY), Zooplankton (ZOO), Particulate Organic Matter (detritus, or POM), Dissolved Organic Matter (DOM), and Iron Nutrient (FE). The material flow and interaction of the compartments is illustrate by Fig. 1.

Each compartment has its own governing equations, which relate to other compartments. Let $[\cdot]$ denote the concentration of various quantities, we have the follow-

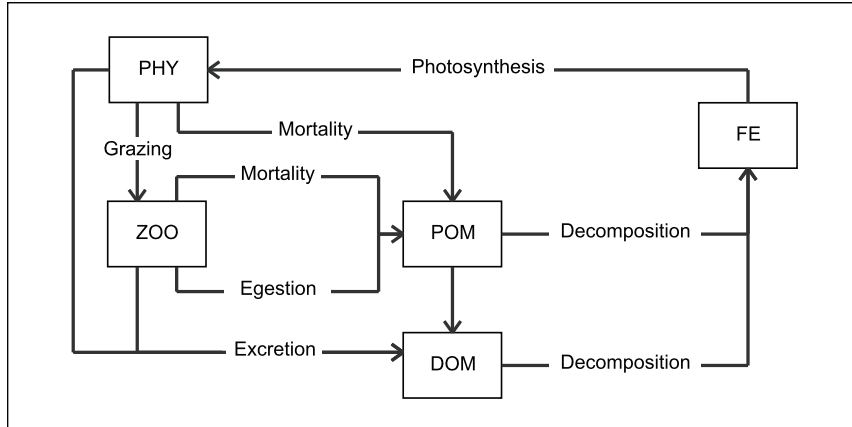


Figure 1: Diagram of compartments.

ing equations to govern the evolution of species in each compartment

$$\begin{aligned} \frac{\partial[\text{PHY}]}{\partial t}(z, t) = & \text{Photosynthesis}([\text{PHY}], z, t) - \text{Excretion}_{\text{PHY}}([\text{PHY}], z, t) \\ & - \text{Mortality}_{\text{PHY}}([\text{PHY}], z, t) - \text{Grazing}([\text{PHY}], [\text{ZOO}], z, t) \\ & + \text{Diffusion}([\text{PHY}], z, t) + \text{Sinking}([\text{PHY}], z, t), \end{aligned} \quad (2.1a)$$

$$\begin{aligned} \frac{\partial[\text{ZOO}]}{\partial t}(z, t) = & \text{Grazing}([\text{PHY}], [\text{ZOO}], z, t) - \text{Excretion}_{\text{ZOO}}([\text{PHY}], [\text{ZOO}], z, t) \\ & - \text{Egestion}_{\text{ZOO}}([\text{PHY}], [\text{ZOO}], z, t) - \text{Mortality}_{\text{ZOO}}([\text{ZOO}], z, t) \\ & + \text{Diffusion}([\text{ZOO}], z, t) + \text{Sinking}([\text{ZOO}], z, t), \end{aligned} \quad (2.1b)$$

$$\begin{aligned} \frac{\partial[\text{POM}]}{\partial t}(z, t) = & \text{Mortality}_{\text{PHY}}([\text{PHY}], z, t) + \text{Mortality}_{\text{ZOO}}([\text{ZOO}], z, t) \\ & + \text{Egestion}_{\text{ZOO}}([\text{PHY}], [\text{ZOO}], z, t) \\ & - \text{POMtoDOM}([\text{POM}], z, t) - \text{POMtoNH4}([\text{POM}], z, t) \\ & + \text{Diffusion}([\text{POM}], z, t) + \text{Sinking}([\text{POM}], z, t), \end{aligned} \quad (2.1c)$$

$$\begin{aligned} \frac{\partial[\text{DOM}]}{\partial t}(z, t) = & \text{Excretion}_{\text{PHY}}([\text{PHY}], z, t) + \text{Excretion}_{\text{ZOO}}([\text{PHY}], [\text{ZOO}], z, t) \\ & + \text{POMtoDOM}([\text{POM}], z, t) - \text{DOMtoNH4}([\text{DOM}], z, t) \\ & + \text{Diffusion}([\text{DOM}], z, t) + \text{Sinking}([\text{DOM}], z, t), \end{aligned} \quad (2.1d)$$

$$\begin{aligned} \frac{\partial[\text{FE}]}{\partial t}(z, t) = & [-\text{Photosynthesis}([\text{PHY}], z, t) \\ & + \text{POMtoNH4}([\text{POM}], z, t) + \text{DOMtoNH4}([\text{DOM}], z, t)] \times \text{FeN} \\ & + \text{Diffusion}([\text{FE}], z, t) + \text{Sinking}([\text{FE}], z, t). \end{aligned} \quad (2.1e)$$

In the following subsections, we provide more detailed explanations on the dynamics included in these equations.

2.1.1 Phytoplankton

The primary production of phytoplankton relies on photosynthesis, i.e.,

$$\begin{aligned} & \text{Photosynthesis}([\text{PHY}], z, t) \\ &= p_{\max} \times \exp(k_{\text{temp}} T(z, t)) \times \frac{I([\text{PHY}], [\text{ZOO}], z, t)}{I_{\text{opt}} \exp\left(1 - \frac{I([\text{PHY}], [\text{ZOO}], z, t)}{I_{\text{opt}}}\right)} \times \frac{[\text{FE}]}{[\text{FE}] + H_{\text{FE}}} \times [\text{PHY}], \end{aligned} \quad (2.2)$$

which in HNLC areas is light- and iron-limited. Note that nitrate and ammonium are not accounted for, since the main concern is iron dependence. Light intensity at depth is modeled by Beer-Lambert's law,

$$I([\text{PHY}], [\text{ZOO}], z, t) = I_{\text{in}} \times \exp\left(-|z|\Lambda + k \int_0^z [\text{PHY}] + k \int_0^z [\text{ZOO}]\right), \quad (2.3)$$

where self shading due phytoplankton, zooplankton, and detritus are all accounted for. Light intensity at the surface is modeled as a sinusoid function, taking into account the annual oscillatory nature of available light. Excretion is assumed to be proportional to photosynthesis, given by

$$\text{Excretion}_{\text{PHY}}([\text{PHY}], z, t) = \gamma \times \text{Photosynthesis}([\text{PHY}], z, t). \quad (2.4)$$

The mortality rate of phytoplankton is described as by Steele and Henderson [11]

$$\text{Mortality}_{\text{PHY}}([\text{PHY}], z, t) = M_{\text{PHY}} \times \exp(k_{M_{\text{PHY}}} T(z, t)) \times [\text{PHY}]^2, \quad (2.5)$$

a quadratic function with respect to concentration.

2.1.2 Zooplankton

Zooplankton grazing process is modeled as an Ivlev equation with phytoplankton concentration serving as the resource, given by

$$\text{Grazing}([\text{PHY}], [\text{ZOO}], z, t) = \max\left(\begin{array}{c} 0 \\ \left(\begin{array}{c} [\text{ZOO}] \times \text{Gr}_{\max} \times \exp(k_{\text{Gr}} T(z, t)) \\ \times \exp\left[1 - \exp(\lambda(\text{Gr}_{\min} - [\text{PHY}]))\right] \end{array} \right) \end{array}\right). \quad (2.6)$$

So long as phytoplankton stocks are above a threshold value, zooplankton will continue to graze. Excretion and egestion are modeled in a similar way to phytoplankton excretion,

$$\text{Excretion}_{\text{ZOO}}([\text{PHY}], [\text{ZOO}], z, t) = (\alpha - \beta) \times \text{Grazing}([\text{PHY}], [\text{ZOO}], z, t), \quad (2.7a)$$

$$\text{Egestion}_{\text{ZOO}}([\text{PHY}], [\text{ZOO}], z, t) = (1 - \alpha) \times \text{Grazing}([\text{PHY}], [\text{ZOO}], z, t), \quad (2.7b)$$

both being proportional to the primary production of zooplankton (grazing). In addition, zooplankton mortality rate

$$\text{Mortality}_{\text{ZOO}}([\text{ZOO}], z, t) = M_{\text{ZOO}} \times \exp(k_{M_{\text{ZOO}}} T(z, t)) \times [\text{ZOO}]^2, \quad (2.8)$$

is essentially the same as phytoplankton mortality rate (Eqs. (2.5)).

2.1.3 Detritus, dissolved organic matter, and iron

Detritus, or particulate organic matter (POM), results from mortality (Eqs. (2.5), and (2.8)), as well as zooplankton egestion (Eq. (2.7b)), and provide the primary mechanism for recycling fixed iron into biologically available iron. Dissolved organic matter (DOM) results from the decay of detritus as well as phytoplankton and zooplankton excretion. To account for iron, a constant iron/nitrogen ratio between the two resources is assumed in all compartments [1,2]. The iron/nitrogen ratio is also the ratio between recycled iron and ammonium [9]. POM decays into both ammonium, given by

$$\text{POMtoNH}_4([\text{POM}], z, t) = R_{\text{decom}} \exp(k_{R_{\text{decom}}} T(z, t)) [\text{POM}], \quad (2.9)$$

and dissolved organic matter (DOM)

$$\text{POMtoDOM}([\text{POM}], z, t) = R_{\text{decom}} \exp(k_{R_{\text{decom}}} T(z, t)) [\text{POM}]. \quad (2.10)$$

DOM will then decay additionally into ammonium

$$\text{DOMtoNH}_4([\text{DOM}], z, t) = R_{\text{decom}} \exp(k_{R_{\text{decom}}} T(z, t)) [\text{DOM}], \quad (2.11)$$

but as a separate compartment than POM. Thus there are two pathways for biological ammonium (and iron) to recycle in the system. The ratio of iron to nitrogen is accounted for in governing equation for iron in the model (Eq. (2.1e)). Note that ammonium is only an important inhibitor in high nitrogen areas, and thus is not included in the model.

In addition to biological processes, iron enters the system through atmospheric flux, with a coverage of roughly $20 \mu\text{mol}/\text{m}^2\text{year}$, and exits the system through scavenging of dissolved iron by other sinking particles. Thus we have incorporated the scavenging model adapted from KKYS-Fe

$$\text{Scavenging}(z, t) = \begin{cases} [\text{Fe}] > 0.6\text{nM}, & (2.74 \times 10^{-5} \times 0.6) + (0.0274 \times ([\text{Fe}] \\ & + 0.6)) \times \frac{([\text{Fe}] - 0.6)}{([\text{Fe}] + 1.4)}, \\ [\text{Fe}] \leq 0.6\text{nM}, & 2.74 \times 10^{-5} \times [\text{Fe}]. \end{cases} \quad (2.12)$$

An important consideration is that by incorporating this scavenging, the system is open and scavenging provides a negative feedback for iron fertilization.

2.1.4 Diffusion and sinking

Turbulent diffusion is described by Fick's law of diffusion in three dimensions

$$\text{Diffusion}(C, t) = \nabla(D\nabla C), \quad (2.13)$$

and in the water column

$$\text{Diffusion}_{1D}(C, z, t) = D \frac{\partial^2 C}{z^2}. \quad (2.14)$$

Sinking simply refers to the apparent sinking velocity of plankton species, as well as detritus

$$\text{Sinking}(C, z, t) = -v \frac{\partial C}{\partial z}. \quad (2.15)$$

2.2 Simulation of the system

The final mathematical model results in a coupled system of multiple partial differential equations. However, due to the self shading characteristic, the equations also include integrals. The solution, proposed by [5], was to discretize in space (keeping the ordinary differential equations (ODEs) continuous in time), allowing the spatial integral portion of the problem to become a discrete approximation. This discretization transforms the problem into a system of ODEs, which are solved numerically using a standard time stepping scheme.

The water column is first divided into cells. Each cell has its own approximation of each of the compartments (PHY, ZOO, POM, DOM, FE) with an ODE describing the time progression of each. Then, through the methods described by Hirsch, we discretize the diffusive term by the second-order centered difference formula, and the sinking term by a third-order upwind scheme. The reason for the more complex discretization of sinking is due to the flow of information (in this case, plankton): by using more information is used from the plankton source and putting less emphasis on plankton sinks.

2.2.1 Initial conditions

All compartments were taken to have a constant initial density with respect to depth. Initial phytoplankton density was set to $0.1 \mu\text{mol}/\text{m}^3$ and initial zooplankton density was $0.01 \mu\text{mol}/\text{m}^3$. The initial POM and DOM densities were set to zero, and iron density was set to $0.6 \times 10^{-4} \text{nmol}/\text{m}^3$. Environmental variables used are supplied in Table 1.

2.2.2 Boundary conditions

Two distinct sets of boundary conditions were explored:

Open System There is no flux of material at either end of the water column, except for atmospheric iron flux, which introduces iron into the system at a constant rate. Iron may also leave the system through scavenging (Eq. (2.12)).

Closed System Iron is completely conserved in the system; the system resembles laboratory environment, as well as giving an "idealized" look at how the system evolves if it is constantly fertilized.

2.2.3 Initialization and simulation

As we are mainly concerned with the equilibrium state of the system (i.e., long term benefits) after the addition of iron, the simulation performs a "spin-up" integration

Table 1: Environmental variables [6, 9].

Variable	Value	Description
z_m	500 m	Relative depth of water column being simulated
z_T	300 m	Relative depth of thermocline
D	432 m ² /day	Turbulent diffusivity
D_T	43.2 m ² /day	Diffusivity below thermocline
k_{temp}	0.63 /°C	Temperature dependence of photosynthesis
Λ	0.035 /m	Background attenuation of ocean water.
I_{in}	120 W/m ²	Maximum incident light intensity at surface
I_{opt}	80 W/m ²	Optimum light intensity for photosynthesis
k	0.028 L/ μ mol N m	Self Shading of plankton, zooplankton, and detritus
γ	0.135	Coefficient of excretion for phytoplankton
v_{PHY}	0.36 m/day	Vertical sinking velocity of phytoplankton
p_{max}	0.5 /day	Maximum photosynthetic productivity of phytoplankton
M_{PHY}	0.028 L/ μ mol N day	Mortality rate of phytoplankton (0°C)
$k_{M_{PHY}}$	0.0693 /°C	Temperature Coefficient for phytoplankton mortality
$G_{r_{max}}$	0.30 /day	Maximum Grazing (0°C)
k_{Gr}	0.0693 /°C	Temperature Coefficient for zooplankton grazing
λ	1.4 L/ μ mol N day	Ivlev constant
$G_{r_{min}}$	0.043 μ mol N/L	Lower threshold of phytoplankton density for grazing to occur
α	0.7	Efficiency of zooplankton grazing
β	0.3	Zooplankton growth rate due to grazing
M_{ZOO}	0.0585 L/ μ mol N day	Mortality rate of zooplankton at 0°C
$k_{M_{ZOO}}$	0.0693 /°C	Temperature coefficient for zooplankton mortality
v_{POM}	10m/day	Sinking velocity of detritus
K_{FE}	0.58 nmol	Half saturation constant of iron for photosynthesis
FE_{atm}	10 mmol/m ² year	Atmospheric iron flux onto the water column
FeN	0.044 nmol/ μ mol	Iron to nitrogen ratio in phytoplankton

over a period of 3 years, to bring the system close to its equilibrium state. Once at this quasi-equilibrium state, a large amount of iron is added to the surface layer, to simulate the effects of iron fertilization. This effect is recorded and the system is allowed to reach equilibrium again. This process was repeated until the maximum threshold for plankton growth was reached.

3 Results

The combined results from three different simulations (an open system, a closed system, and a system without predators) are shown in Figs. 8, 9 (as blue, red, and green respectively), 4, and 2. Before discussing the simulation results in detail, a few remarks are in order. From the results obtained, it is apparent that while iron fertilization has a temporary benefit of dramatically increasing phytoplankton stock, this temporary population boom is rapidly counteracted by the proliferation of predator species, namely zooplankton, in the system. After this the system attains a new equilibrium. This new equilibrium depends on the assumption whether the system is open (iron may leave the system to restore equilibrium), or closed (the system reaches a new equilibrium around the iron concentration), and the interaction between phytoplankton and predator species.

3.1 Open system

In an open system (Fig. 8, blue), the new biomass introduced by iron fertilization cannot (and indeed, does not) remain in the system indefinitely, as the iron sequestered by biological activity is still slowly leached out by scavenging, unless balanced by an external source of iron (atmospheric iron is insufficient). In our simulation, the zooplankton reaction to the iron fertilization takes roughly three weeks, and zooplankton population peaks at one month, exhausting the majority of the phytoplankton stock generated by iron fertilization. A second, slower systemic reaction occurs when the iron levels in the column continue to drop, decreasing the carrying capacity of the system. This second wave is manifested as a less extreme decrease in phytoplankton stock (with a time period ranging from 1 month to 3 months). The relaxation period for iron concentration is roughly 150 days, or 5 months. In an open system the increased carbon sequestering can only be from continued fertilization.

3.2 Closed system

If the iron levels could be maintained, the potential for growth would be dramatically increased, as evidenced by Figs. 2 and 4. The resulting increase in phytoplankton productivity would be quite large, as shown by the significant difference in phytoplankton population between open and closed systems in the first column in Figs. 8 and 9. In addition, the relaxation period of the system is very short, usually taking only a few weeks. This case is less interesting as it does not occur naturally, but is useful for reference purposes as to the direct relation between iron concentration and photosynthetic activity.

Interestingly, even in a closed system, the equilibrium state does not shift much with the introduction of additional iron. Doubling the iron in the system, the overall phytoplankton population only increases by $\sim 10\%$. This may explain the apparent ineffectiveness that researchers experimenting with iron fertilization are seeing. In a realistic environment, extra production is greatly buffered by natural responses. As such it is best to think of the impact of iron fertilization within the time frame of a few months after fertilization, when the phytoplankton yield is greatest.

3.3 Predator-less system

Finally, Fig. 8 (green) shows an open system without the presence of zooplankton. Due to the slower iron uptake process, the phytoplankton bloom has a shorter duration than in a system which includes predators. This allows for scavenging of dissolved iron to occur more rapidly due to (Eq. (2.12)). The shorter relaxation time is owed to the role the predators play in increasing the effect of iron fertilization. Firstly, by consuming phytoplankton, zooplankton act as a reservoir for iron while freeing up "space" by eliminating competition for the light sensitive production of phytoplankton. Secondly, by increasing the mortality rate of phytoplankton through grazing, more iron is also retained via detritus and DOM. Without the predators the system

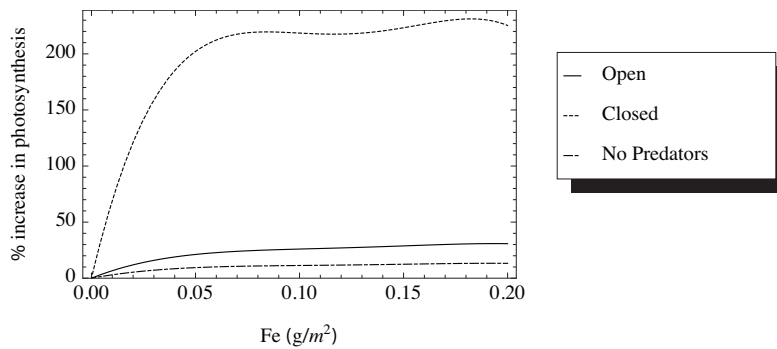


Figure 2: Ratio of increase in photosynthesis of different simulations.

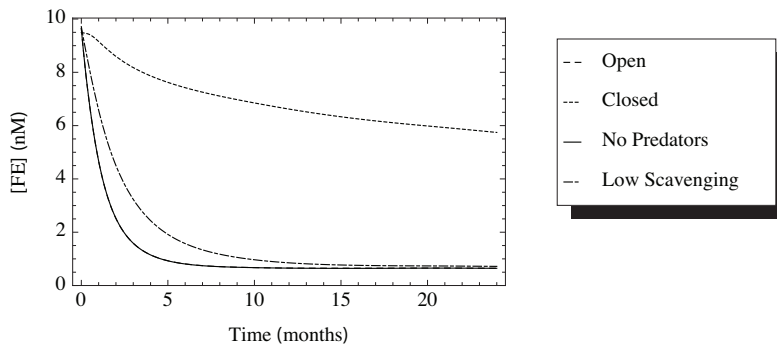


Figure 3: Average iron concentration within the thermocline. When scavenging is inhibited (Purple), the relaxation time of the system is substantially longer. Note that iron tends to leave the thermocline in a closed system sinking to lower portions of the mixed layer (red curve). Note: the "Open" and "No Predator" systems are virtually identical, and their curves are coincident in this plot.

no longer benefits from an increased storage capacity for biologically available iron. However, without predators the bloom is allowed to develop more fully, resulting in overall the greatest amount of photosynthetic activity, as seen in Figs. 2 and 4.

3.4 Effect of iron scavenging

One of the most important issues that iron fertilization faces is the rate at which extra iron is scavenged in the system. In cases where rate of iron scavenging is decreased (Fig. 3), the relaxation period is much greater and the resultant increase in photosynthetic activity is more significant.

3.5 Carbon sequestering

Photosynthetic activity and Carbon flux through the thermocline are used as performance indicators for the CO_2 uptake of the bloom, and are used to compare model runs in this paper. Since carbon fixation only occurs from photosynthesis in phytoplankton blooms, the amount of carbon sunk must also be closely related to the photosynthetic activity. Thus it is beneficial to look at the rate of photosynthesis as well

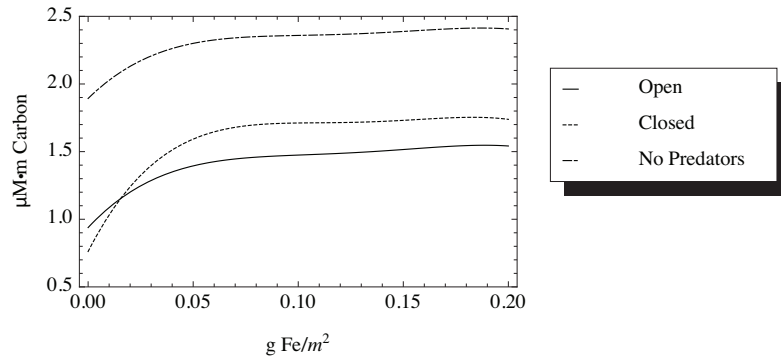


Figure 4: Effect of turbulent diffusivity on average flux of carbon across the thermocline, from fertilization to 5 months after (effective duration of fertilization).

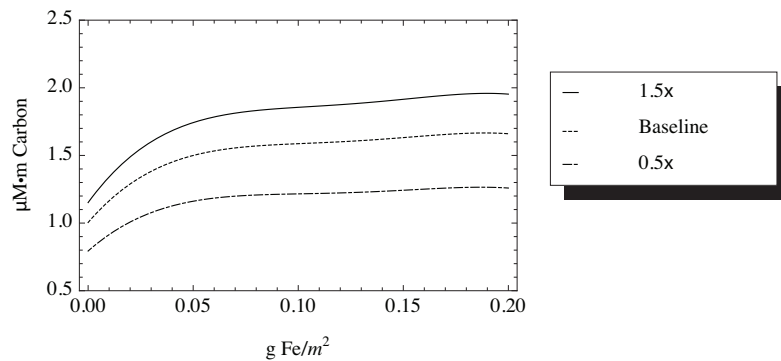


Figure 5: Effect of turbulent diffusivity on the average flux of carbon across the thermocline, from fertilization to 5 months after.

as phytoplankton population. The second metric for performance is the movement of carbon across the thermocline (Fig. 4). Once carbon has moved below the thermocline, it is much more likely to be retained by the system, as natural forces such as turbulent mixing and reincorporation into biomass are greatly reduced.

3.6 Sensitivity analysis

Sensitivity analysis was carried out to determine the impact of critical simulation parameters on carbon sequestering.

Diffusivity (Fig. 5) was found to have significant effect on phytoplankton productivity and the rate of carbon sequestering. Phytoplankton bloom density was found to increase with greater turbulent diffusion, as the phytoplankton blooms were increasingly able to overcome sinking. Thus, it may be interesting to investigate a more fine-grained approach to modelling the spatial variation in diffusivity, to better assess its impact on real-world carbon sequestering.

The depth of the thermocline governed the "cut-off" region of biological activity. As can be seen in Fig. 6, overall carbon sequestering is lowered in deeper thermoclines. This is not due to a decrease in phytoplankton population, as blooms are actually denser in deep thermoclines. In the case of a deep thermocline, most sink-

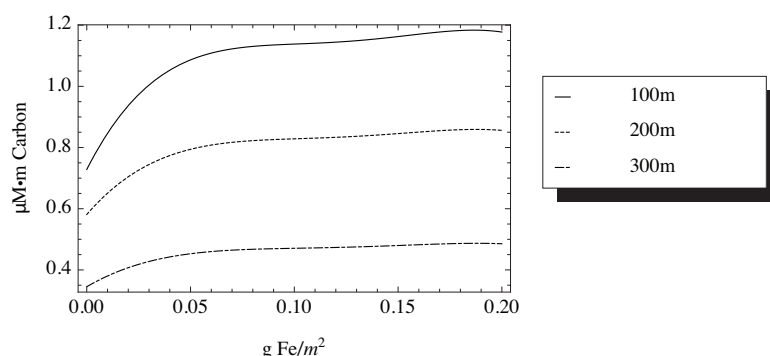


Figure 6: Effect of thermocline depth on the average flux of carbon across the thermocline, from fertilization to 5 months after.

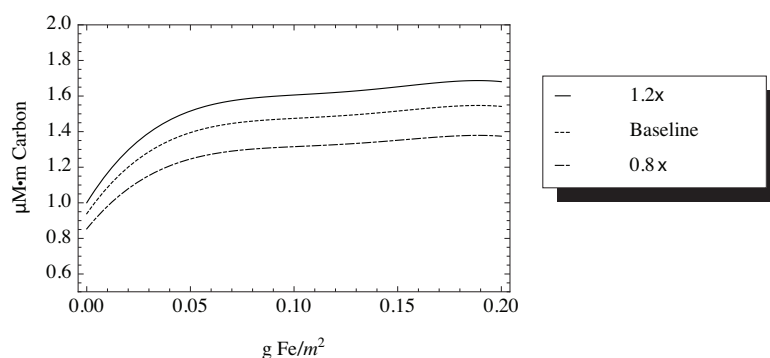


Figure 7: Effect of incident sunlight intensity on the average flux of carbon across the thermocline, from fertilization to 5 months after.

ing DOM is reincorporated before it leaves the thermocline. In the case of a shallow thermocline, sinking DOM has a higher chance of passing the thermocline before it is reincorporated.

The effect of light intensity was fairly predictable; phytoplankton bloom size and productivity scales linearly to light intensity (Fig. 7).

4 Conclusions

The proper application of iron fertilization will see utility either in seeding phytoplankton blooms in an area, or in the case of extreme iron deficiencies (such as in Antarctic oceans), populating a region otherwise incapable of sustaining phytoplankton. For researchers a pressing issue with carrying out continued fertilization is the difficulty of measuring actual CO_2 uptake of phytoplankton blooms. The best that can be measured, such as in the LOHAFEX expedition, were the density of local marine biology and chlorophyll concentration within the region. The difficulty is that these values only provide an estimate, while a real metric would allow for the collaborative efforts of international organizations, countries, and private companies to appoint carbon quotas for operations.

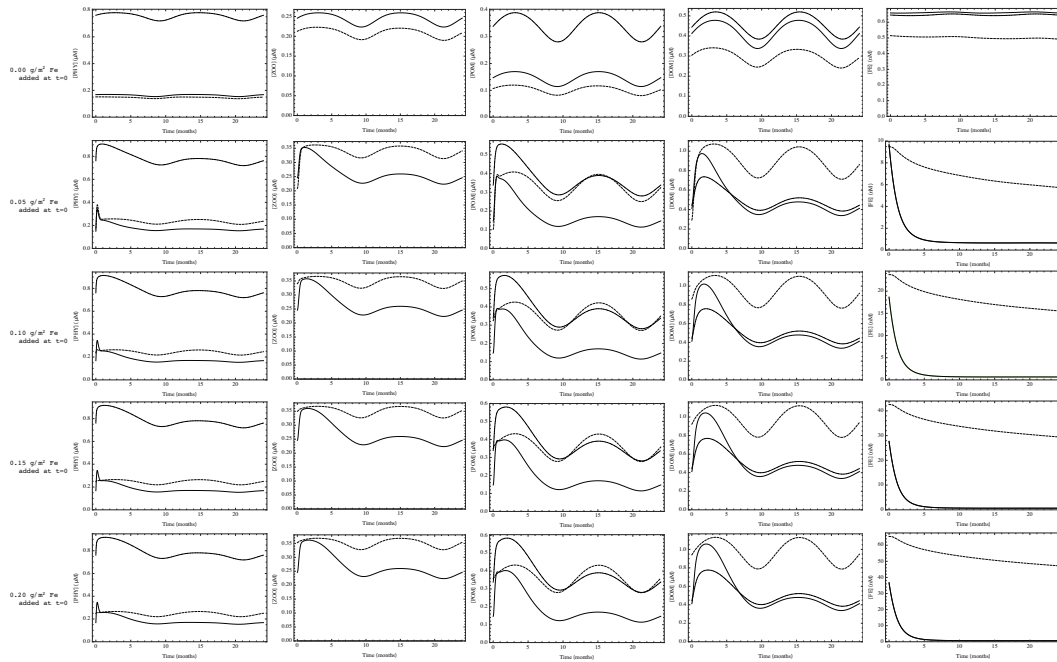


Figure 8: Average values within euphotic zone vs. time. Blue, red, and green represent open, closed, and predator-less systems.

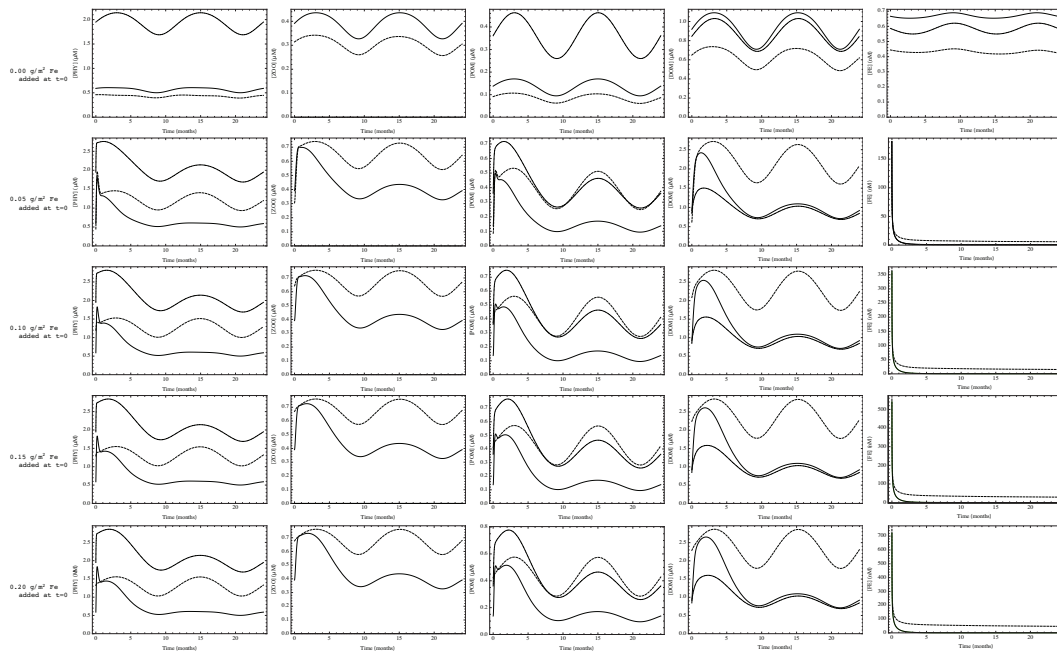


Figure 9: Surface Profiles vs. time.

The actual mechanisms by which fixed carbon dioxide sinks or returns to the atmosphere has not been explored in this paper, and inclusion into the model would provide further insight into the dynamics at which plankton sequester carbon into the ocean. The next step would be to examine these mechanisms. Larger predator species (such as krill, fish, and other organisms which rely on phytoplankton) and multiple competing species of phytoplankton should be incorporated, if only to see how iron fertilization affects the relative proportion of separate species, and if fertilization would result in the proliferation of one particular species. Destabilizing the natural equilibrium may have far reaching consequences, potentially reducing the biodiversity of the system. As the system eventually should return to natural equilibrium, reshuffling the biological makeup would be most undesirable.

Iron fertilization seems to have relatively little long-term or permanent effects on the ecology of plankton blooms, and the actual benefit of large scale fertilization remains to be seen in major HNLC oceans. Only as more expeditions are made and realistic models are developed, will more data be made readily available for furthering the understanding of the effects of iron fertilization on plankton growth dynamics and its function as a biological carbon pump.

References

- [1] W. W. GREGG, *Tracking the SeaWiFS record with a coupled physical/biogeochemical/radiative model of the global oceans*, Deep. Sea. Res. II., 49 (2001), pp. 81–105.
- [2] W. W. GREGG, P. GINOUX, P. S. SCHOPF, AND N. W. CASEY, *Phytoplankton and iron: validation of a global three-dimensional ocean biogeochemical model*, Deep. Sea. Res. II., 50 (2003), pp. 3143–3169.
- [3] J. HUISMAN, M. ARRAYAS, AND U. EBERT, *How do sinking phytoplankton species manage to persist?*, Am. Nat., 159 (2002), pp. 245–254.
- [4] J. HUISMAN, AND B. SOMMEJER, *Population dynamics of sinking phytoplankton in light-limited environments: simulation techniques and critical parameters*, J. Sea. Res., 48 (2002), pp. 83–96.
- [5] J. HUISMAN, AND B. P. SOMMEIJER, *Simulation Techniques for the Population Dynamics of Sinking Phytoplankton in Light Limited Environments*, 2002.
- [6] M. KAWAMIYA, M. KISHI, Y. YAMANAKA, AND N. SUGINOHARA, *An ecological-physical coupled model applied to station papa*, J. Oceanography., 51 (1995), pp. 635–664.
- [7] M. KISHI, H. MOTONO, M. KASHIWAI, AND A. TSUDA, *An ecological-physical coupled model with ontogenetic vertical migration of zooplankton in the northwestern pacific*, J. Oceanography., 57 (2001), pp. 499–507.
- [8] L. LIPPSETT, K. MADIN, AND A. NEVALA, *WHOI: Oceanus: Fertilizing the Ocean with Iron*, <http://www.whoi.edu/oceanus/viewArticle.do?id=34167§ionid=1000>.
- [9] T. OKUNISHI, M. J. KISHI, Y. ONO, AND T. YAMASHITA, *A lower trophic ecosystem model including iron effects in the Okhotsk sea*, Cont. Shelf. Res., 27 (2007), pp. 2080–2098.
- [10] J. ROACH, *Can Iron-Enriched Oceans Thwart Global Warming?*, http://news.national-geographic.com/news/2004/06/0609_040609_carbonsink.html.
- [11] J. H. STEELE, AND E. W. HENDERSON, *The role of predation in Plankton models*, J. Plankton. Res., 14 (1992), pp. 157–172.